

Introduction to topology in electronic structure of crystalline solids

Tomáš Rauch

IFTO, FSU Jena

Schedule

- ▶ 24.03. Introduction into topological insulators
- ▶ 14.04. Topological insulators in two and three dimensions
- ▶ 21.04. Calculation of topological invariants of realistic materials
- ▶ 28.04. Role of spin-orbit coupling, band inversions and experimental evidence
- ▶ 05.05. (Hybrid) Wannier functions
- ▶ 12.05. Higher-order topological insulators, topological metals, skyrmions, Majorana fermions
- ▶ TBA Applications / Unanswered topics?

Literature

- ▶ D. Vanderbilt, Berry phases in electronic structure theory
- ▶ B. A. Bernevig, Topological insulators and topological superconductors
- ▶ J. K. Asboth, L. Oroszlany, A. Pályi, A short course on topological insulators

Higher-order topological insulators (HOTIs)¹

¹Schindler *et al.*, Science Advances 4, eaat0346 (2018)

Higher-order topological insulators (HOTIs)¹

- ▶ so far: TIs periodic in D dimensions \rightarrow surface states on a $D - 1$ dimensional surface
 - ▶ e.g.: 2D TIs with edge states at 1D edges

¹Schindler *et al.*, Science Advances 4, eaat0346 (2018)

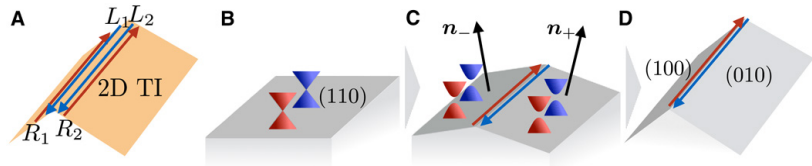
Higher-order topological insulators (HOTIs)¹

- ▶ so far: TIs periodic in D dimensions \rightarrow surface states on a $D - 1$ dimensional surface
 - ▶ e.g.: 2D TIs with edge states at 1D edges
- ▶ generalization: TIs periodic in D dimensions \rightarrow surface states on a $D - n$ dimensional surface
 - ▶ TIs of order n : "higher-order TIs"
 - ▶ e.g.: 2D TIs with corner states at 0D corners $\rightarrow n = 2$

¹Schindler *et al.*, Science Advances 4, eaat0346 (2018)

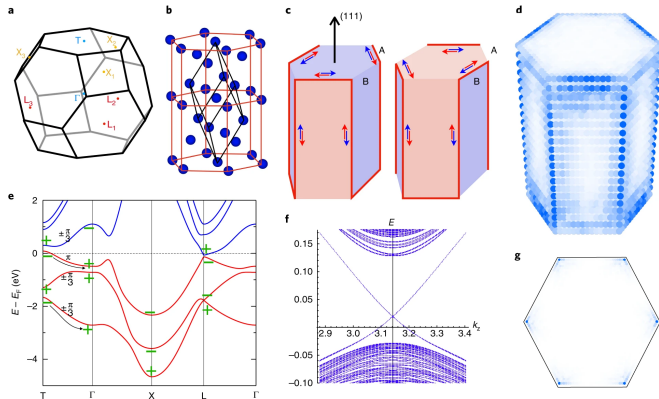
Higher-order topological insulators (HOTIs)¹

- ▶ so far: TIs periodic in D dimensions \rightarrow surface states on a $D - 1$ dimensional surface
 - ▶ e.g.: 2D TIs with edge states at 1D edges
- ▶ generalization: TIs periodic in D dimensions \rightarrow surface states on a $D - n$ dimensional surface
 - ▶ TIs of order n : "higher-order TIs"
 - ▶ e.g.: 2D TIs with corner states at 0D corners $\rightarrow n = 2$
 - ▶ e.g.: 3D TIs with hinge states at 1D hinges $\rightarrow n = 2$
 \rightarrow connecting adjacent insulating surfaces



¹Schindler *et al.*, Science Advances 4, eaat0346 (2018)

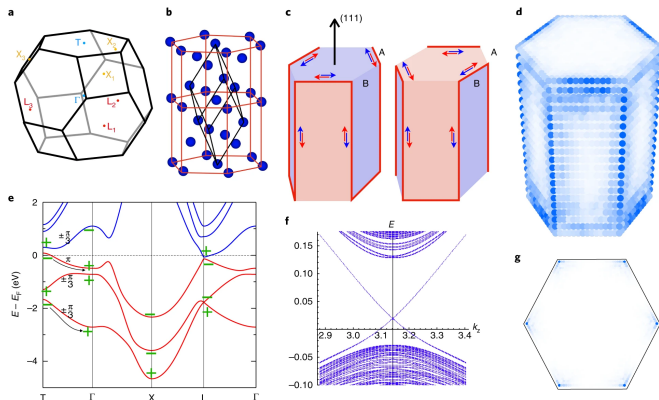
HTOI example: Bismuth²



²Schindler *et al.*, Nature **14**, 918 (2018)

HTOI example: Bismuth²

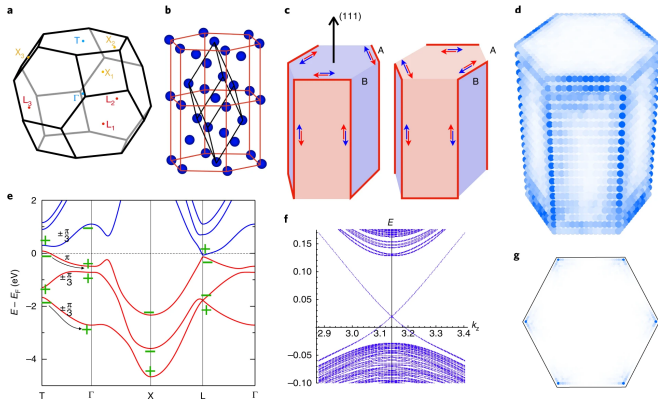
- ▶ topological invariant from combined C_3 and I symmetry
 - ▶ symmetry eigenvalues at TRIMs



²Schindler et al., Nature 14, 918 (2018)

HTOI example: Bismuth²

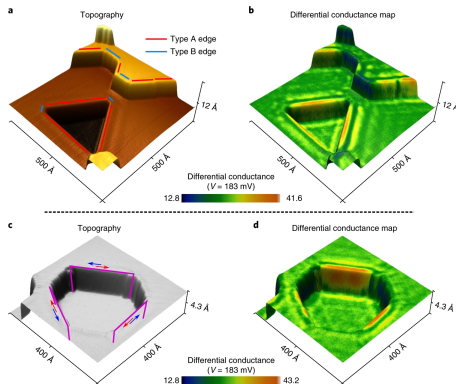
- ▶ topological invariant from combined C_3 and I symmetry
 - ▶ symmetry eigenvalues at TRIMs
- ▶ two types of insulating surfaces
 - ▶ metallic “hinge states” at hinges A connecting different surfaces



²Schindler et al., Nature 14, 918 (2018)

HOTI example: Bismuth²

- ▶ topological invariant from combined C_3 and I symmetry
 - ▶ symmetry eigenvalues at TRIMs
- ▶ two types of insulating surfaces
 - ▶ metallic “hinge states” at hinges A connecting different surfaces



²Schindler et al., Nature 14, 918 (2018)

Topological metals

Topological metals

- ▶ ideally semimetals with symmetry-protected band crossings at E_F

Topological metals

- ▶ ideally semimetals with symmetry-protected band crossings at E_F
- ▶ transport properties different from parabolic bands

Topological metals

- ▶ ideally semimetals with symmetry-protected band crossings at E_F
- ▶ transport properties different from parabolic bands
- ▶ Dirac semimetals
- ▶ Weyl semimetals
- ▶ nodal-line semimetals
- ▶ others...

Dirac semimetals

- ▶ low-energy description: massless Dirac Hamiltonian $H = c\alpha \cdot \mathbf{p}$

³B.-J. Yang and N. Nagaosa, Nature Comms. **5**, 4898 (2014)

⁴B.-J. Yang, T. Morimoto, and A. Furusaki, Phys. Rev. B **92**, 165120 (2015)

⁵Z. Wang *et al.*, Phys. Rev. B **88**, 125427 (2013)

Dirac semimetals

- ▶ low-energy description: massless Dirac Hamiltonian $H = c\alpha \cdot \mathbf{p}$
- ▶ solutions: 4-component spinors, $E = \pm c|\mathbf{p}|$
 - ▶ doubly-degenerate bands (typically TR+I)
 - ▶ linear dispersion close to the crossing point → Dirac point

³B.-J. Yang and N. Nagaosa, Nature Comms. **5**, 4898 (2014)

⁴B.-J. Yang, T. Morimoto, and A. Furusaki, Phys. Rev. B **92**, 165120 (2015)

⁵Z. Wang *et al.*, Phys. Rev. B **88**, 125427 (2013)

Dirac semimetals

- ▶ low-energy description: massless Dirac Hamiltonian $H = c\alpha \cdot \mathbf{p}$
- ▶ solutions: 4-component spinors, $E = \pm c|\mathbf{p}|$
 - ▶ doubly-degenerate bands (typically TR+I)
 - ▶ linear dispersion close to the crossing point \rightarrow Dirac point
- ▶ 2D: Berry phase on a path enclosing the Dirac point $\phi = \pi$
 - ▶ e.g. graphene without SOC

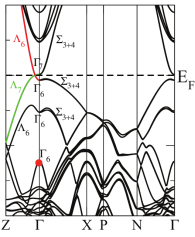
³B.-J. Yang and N. Nagaosa, Nature Comms. **5**, 4898 (2014)

⁴B.-J. Yang, T. Morimoto, and A. Furusaki, Phys. Rev. B **92**, 165120 (2015)

⁵Z. Wang *et al.*, Phys. Rev. B **88**, 125427 (2013)

Dirac semimetals

- ▶ low-energy description: massless Dirac Hamiltonian $H = c\alpha \cdot \mathbf{p}$
- ▶ solutions: 4-component spinors, $E = \pm c|\mathbf{p}|$
 - ▶ doubly-degenerate bands (typically TR+I)
 - ▶ linear dispersion close to the crossing point \rightarrow Dirac point
- ▶ 2D: Berry phase on a path enclosing the Dirac point $\phi = \pi$
 - ▶ e.g. graphene without SOC
- ▶ 3D: Dirac point can be pinned to high-symmetry points / lines by crystalline symmetries³⁴ (different IRREPs can cross each other)



▶ e.g. Cd_3As_2 ⁵

³B.-J. Yang and N. Nagaosa, Nature Comms. **5**, 4898 (2014)

⁴B.-J. Yang, T. Morimoto, and A. Furusaki, Phys. Rev. B **92**, 165120 (2015)

⁵Z. Wang *et al.*, Phys. Rev. B **88**, 125427 (2013)

Weyl semimetals

- ▶ low-energy description: massless Weyl Hamiltonian $H(\mathbf{k}) = v_{ij}k_i\sigma_j$
- ▶ $\sigma_i \dots$ Pauli matrices

⁶M. Berry, Proc. Roy. Soc. London A **392**, 45 (1984)

Weyl semimetals

- ▶ low-energy description: massless Weyl Hamiltonian $H(\mathbf{k}) = v_{ij} k_i \sigma_j$
- ▶ $\sigma_i \dots$ Pauli matrices
- ▶ solution: 2-component spinor, for $v_{ij} = v\delta_{ij}$: $E(\mathbf{k}) = v|\mathbf{k}|$
 - ▶ linear dispersion
 - ▶ only if TR or I is broken

⁶M. Berry, Proc. Roy. Soc. London A **392**, 45 (1984)

Weyl semimetals

- ▶ low-energy description: massless Weyl Hamiltonian $H(\mathbf{k}) = v_{ij} k_i \sigma_j$
- ▶ $\sigma_i \dots$ Pauli matrices
- ▶ solution: 2-component spinor, for $v_{ij} = v \delta_{ij}$: $E(\mathbf{k}) = v|\mathbf{k}|$
 - ▶ linear dispersion
 - ▶ only if TR or I is broken
- ▶ Berry curvature of the bands ($v = \frac{1}{2}$)⁶: $\Omega_{\pm}(\mathbf{k}) = \pm \frac{\mathbf{k}}{2k^3}$
 - ▶ c.f. magnetic field of magnetic monopoles
 - ▶ Weyl points are the only sources (monopoles) of Berry curvature

⁶M. Berry, Proc. Roy. Soc. London A **392**, 45 (1984)

Weyl semimetals

- ▶ low-energy description: massless Weyl Hamiltonian $H(\mathbf{k}) = v_{ij} k_i \sigma_j$
- ▶ $\sigma_i \dots$ Pauli matrices
- ▶ solution: 2-component spinor, for $v_{ij} = v \delta_{ij}$: $E(\mathbf{k}) = v|\mathbf{k}|$
 - ▶ linear dispersion
 - ▶ only if TR or I is broken
- ▶ Berry curvature of the bands ($v = \frac{1}{2}$)⁶: $\Omega_{\pm}(\mathbf{k}) = \pm \frac{\mathbf{k}}{2k^3}$
 - ▶ c.f. magnetic field of magnetic monopoles
 - ▶ Weyl points are the only sources (monopoles) of Berry curvature
- ▶ any closed surface S enclosing the Weyl point (in \mathbf{k} space):

$$C_{\pm}(S) = \frac{1}{2\pi} \oint_S dS \ \hat{\mathbf{n}} \cdot \Omega_{\pm}(\mathbf{k}) = \pm 1$$

- ▶ $C_- \dots$ chirality of the Weyl point (WP)

⁶M. Berry, Proc. Roy. Soc. London A **392**, 45 (1984)

Weyl semimetals

Properties:

Weyl semimetals

Properties:

- ▶ Weyl points must occur in pairs (zero total Chern number)

Weyl semimetals

Properties:

- ▶ Weyl points must occur in pairs (zero total Chern number)
- ▶ Weyl points created/destroyed by pair creation / annihilation

Weyl semimetals

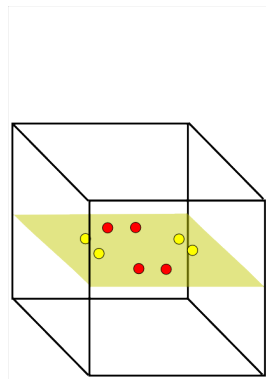
Properties:

- ▶ Weyl points must occur in pairs (zero total Chern number)
- ▶ Weyl points created/destroyed by pair creation / annihilation
- ▶ Surface states: E_F at WP energy

Weyl semimetals

Properties:

- ▶ Weyl points must occur in pairs (zero total Chern number)
- ▶ Weyl points created/destroyed by pair creation / annihilation
- ▶ Surface states: E_F at WP energy
- ▶ bulk Fermi surface: isolated points

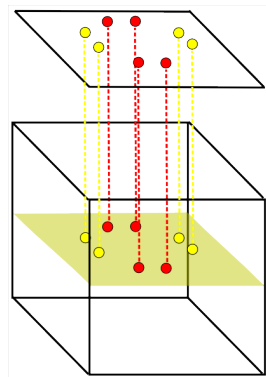


Weyl semimetals

Properties:

- ▶ Weyl points must occur in pairs (zero total Chern number)
- ▶ Weyl points created/destroyed by pair creation / annihilation
- ▶ Surface states: E_F at WP energy

- ▶ bulk Fermi surface: isolated points
- ▶ surface Fermi surface: projected WPs

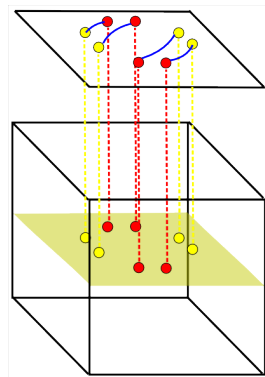


Weyl semimetals

Properties:

- ▶ Weyl points must occur in pairs (zero total Chern number)
- ▶ Weyl points created/destroyed by pair creation / annihilation
- ▶ Surface states: E_F at WP energy

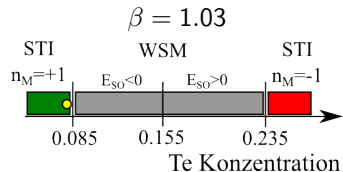
- ▶ bulk Fermi surface: isolated points
- ▶ surface Fermi surface: projected WPs
- ▶ surface Fermi surface: open lines (**Fermi arcs**) connecting pairs of WPs with opposite chirality



Weyl semimetal

Example: strained HgTe_xS_{1-x}⁷

- ▶ varying Te content (x)

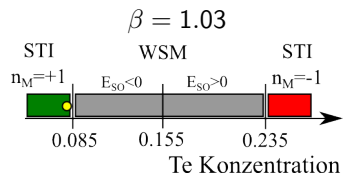


⁷Rauch *et al.*, PRL 114, 236805 (2015)

Weyl semimetal

Example: strained HgTe_xS_{1-x}⁷

- ▶ varying Te content (x)
 - ▶ TI \rightarrow WSM \rightarrow TI

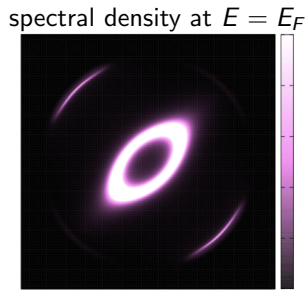
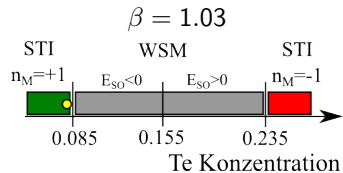


⁷Rauch *et al.*, PRL 114, 236805 (2015)

Weyl semimetal

Example: strained HgTe_xS_{1-x}⁷

- ▶ varying Te content (x)
 - ▶ TI \rightarrow WSM \rightarrow TI
 - ▶ Chern numbers:
yellow: $C = +1$
red: $C = -1$

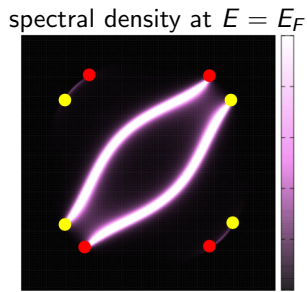
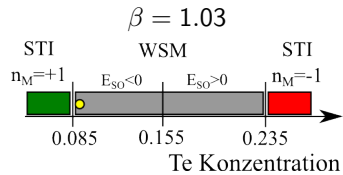


⁷Rauch *et al.*, PRL 114, 236805 (2015)

Weyl semimetal

Example: strained HgTe_xS_{1-x}⁷

- ▶ varying Te content (x)
 - ▶ TI \rightarrow WSM \rightarrow TI
 - ▶ Chern numbers:
yellow: $C = +1$
red: $C = -1$

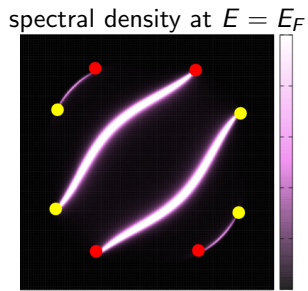
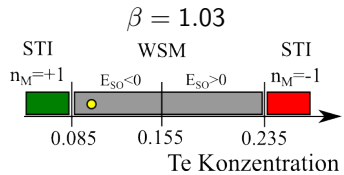


⁷Rauch *et al.*, PRL 114, 236805 (2015)

Weyl semimetal

Example: strained HgTe_xS_{1-x}⁷

- ▶ varying Te content (x)
 - ▶ TI \rightarrow WSM \rightarrow TI
 - ▶ Chern numbers:
yellow: $C = +1$
red: $C = -1$

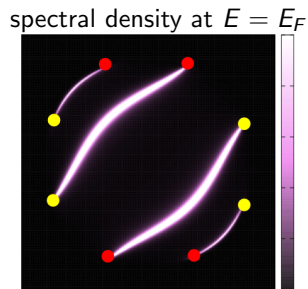
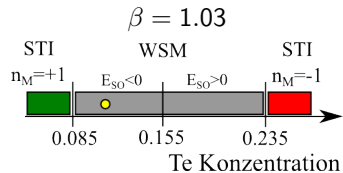


⁷Rauch *et al.*, PRL 114, 236805 (2015)

Weyl semimetal

Example: strained $\text{HgTe}_x\text{S}_{1-x}$ ⁷

- ▶ varying Te content (x)
- ▶ TI \rightarrow WSM \rightarrow TI
- ▶ Chern numbers:
yellow: $C = +1$
red: $C = -1$

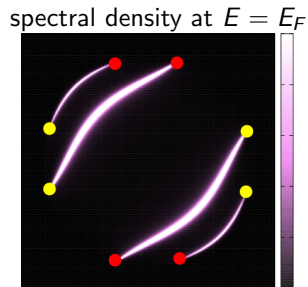
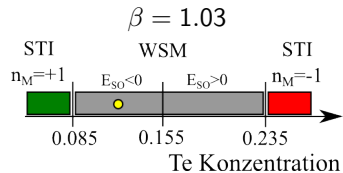


⁷Rauch et al., PRL 114, 236805 (2015)

Weyl semimetal

Example: strained $\text{HgTe}_x\text{S}_{1-x}$ ⁷

- ▶ varying Te content (x)
- ▶ TI \rightarrow WSM \rightarrow TI
- ▶ Chern numbers:
yellow: $C = +1$
red: $C = -1$

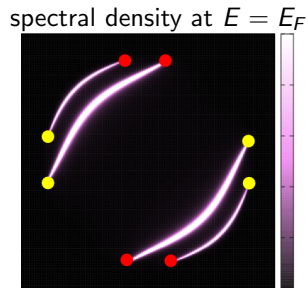
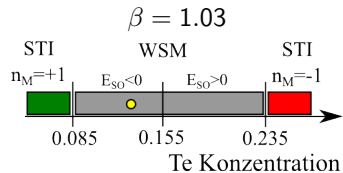


⁷Rauch *et al.*, PRL 114, 236805 (2015)

Weyl semimetal

Example: strained $\text{HgTe}_x\text{S}_{1-x}$ ⁷

- ▶ varying Te content (x)
- ▶ TI \rightarrow WSM \rightarrow TI
- ▶ Chern numbers:
yellow: $C = +1$
red: $C = -1$

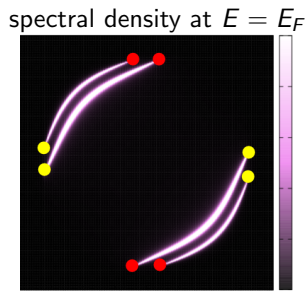
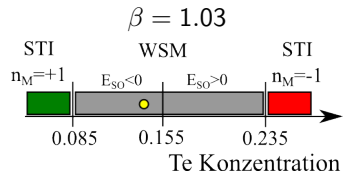


⁷Rauch et al., PRL 114, 236805 (2015)

Weyl semimetal

Example: strained HgTe_xS_{1-x}⁷

- ▶ varying Te content (x)
 - ▶ TI \rightarrow WSM \rightarrow TI
 - ▶ Chern numbers:
yellow: $C = +1$
red: $C = -1$

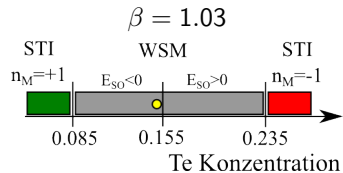


⁷Rauch *et al.*, PRL 114, 236805 (2015)

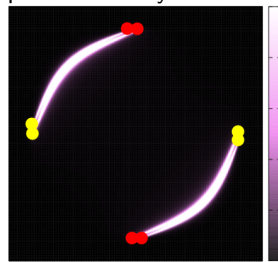
Weyl semimetal

Example: strained $\text{HgTe}_x\text{S}_{1-x}$ ⁷

- ▶ varying Te content (x)
- ▶ TI \rightarrow WSM \rightarrow TI
- ▶ Chern numbers:
yellow: $C = +1$
red: $C = -1$



spectral density at $E = E_F$

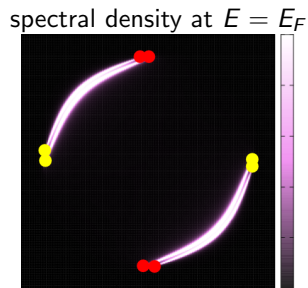
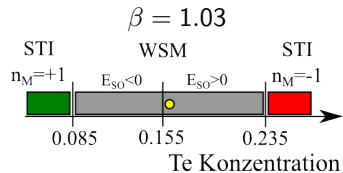


⁷Rauch *et al.*, PRL 114, 236805 (2015)

Weyl semimetal

Example: strained $\text{HgTe}_x\text{S}_{1-x}$ ⁷

- ▶ varying Te content (x)
- ▶ TI \rightarrow WSM \rightarrow TI
- ▶ Chern numbers:
yellow: $C = +1$
red: $C = -1$

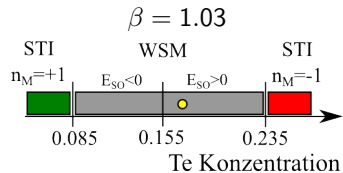


⁷Rauch et al., PRL 114, 236805 (2015)

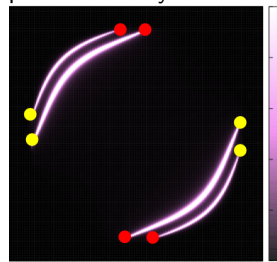
Weyl semimetal

Example: strained $\text{HgTe}_x\text{S}_{1-x}$ ⁷

- ▶ varying Te content (x)
- ▶ TI \rightarrow WSM \rightarrow TI
- ▶ Chern numbers:
yellow: $C = +1$
red: $C = -1$



spectral density at $E = E_F$

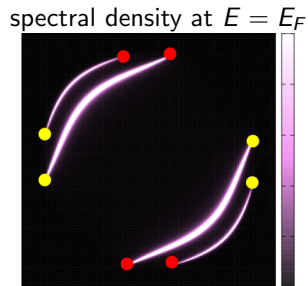
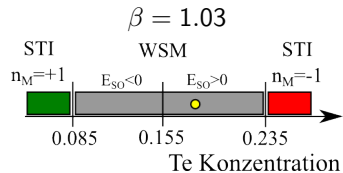


⁷Rauch et al., PRL 114, 236805 (2015)

Weyl semimetal

Example: strained $\text{HgTe}_x\text{S}_{1-x}$ ⁷

- ▶ varying Te content (x)
- ▶ TI \rightarrow WSM \rightarrow TI
- ▶ Chern numbers:
yellow: $C = +1$
red: $C = -1$

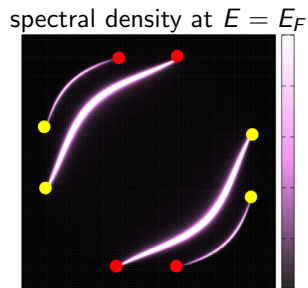
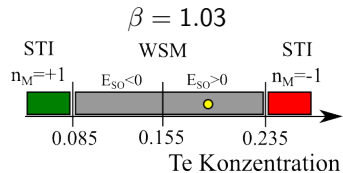


⁷Rauch et al., PRL 114, 236805 (2015)

Weyl semimetal

Example: strained $\text{HgTe}_x\text{S}_{1-x}$ ⁷

- ▶ varying Te content (x)
- ▶ TI \rightarrow WSM \rightarrow TI
- ▶ Chern numbers:
yellow: $C = +1$
red: $C = -1$

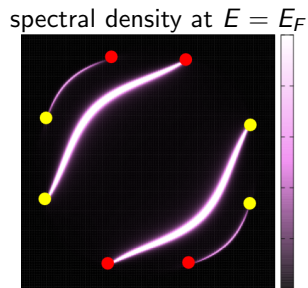
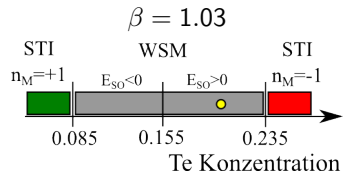


⁷Rauch et al., PRL 114, 236805 (2015)

Weyl semimetal

Example: strained $\text{HgTe}_x\text{S}_{1-x}$ ⁷

- ▶ varying Te content (x)
- ▶ TI \rightarrow WSM \rightarrow TI
- ▶ Chern numbers:
yellow: $C = +1$
red: $C = -1$

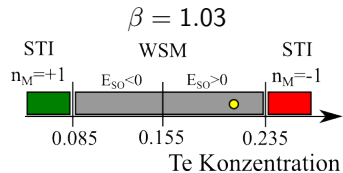


⁷Rauch et al., PRL 114, 236805 (2015)

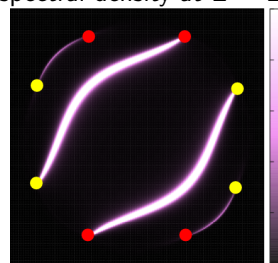
Weyl semimetal

Example: strained $\text{HgTe}_x\text{S}_{1-x}$ ⁷

- ▶ varying Te content (x)
- ▶ TI \rightarrow WSM \rightarrow TI
- ▶ Chern numbers:
yellow: $C = +1$
red: $C = -1$



spectral density at $E = E_F$

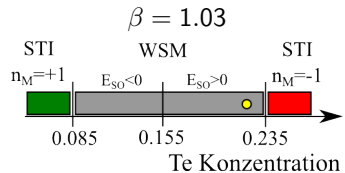


⁷Rauch et al., PRL 114, 236805 (2015)

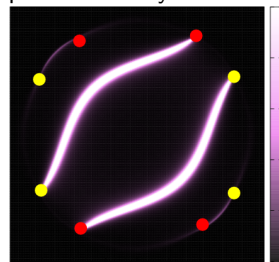
Weyl semimetal

Example: strained $\text{HgTe}_x\text{S}_{1-x}$ ⁷

- ▶ varying Te content (x)
- ▶ TI \rightarrow WSM \rightarrow TI
- ▶ Chern numbers:
yellow: $C = +1$
red: $C = -1$



spectral density at $E = E_F$

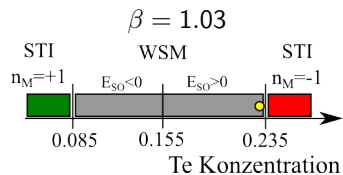


⁷Rauch et al., PRL 114, 236805 (2015)

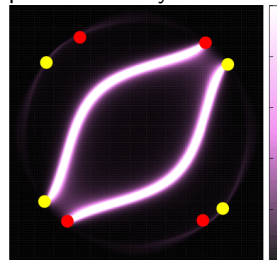
Weyl semimetal

Example: strained $\text{HgTe}_x\text{S}_{1-x}$ ⁷

- ▶ varying Te content (x)
- ▶ TI \rightarrow WSM \rightarrow TI
- ▶ Chern numbers:
yellow: $C = +1$
red: $C = -1$



spectral density at $E = E_F$

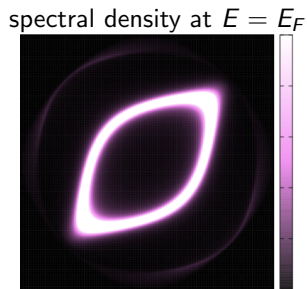
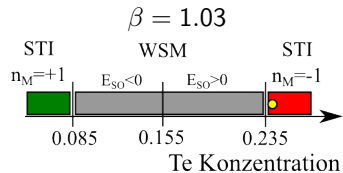


⁷Rauch et al., PRL 114, 236805 (2015)

Weyl semimetal

Example: strained HgTe_xS_{1-x}⁷

- ▶ varying Te content (x)
 - ▶ TI \rightarrow WSM \rightarrow TI
 - ▶ Chern numbers:
yellow: $C = +1$
red: $C = -1$



⁷Rauch *et al.*, PRL 114, 236805 (2015)

Weyl semimetals

Chiral anomaly⁸

⁸Son and Spivak, PRB **88**, 104412 (2013)

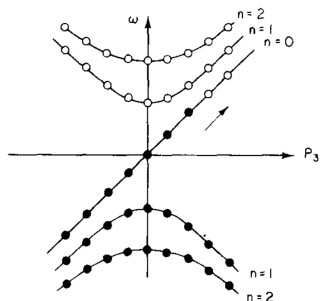
⁹Nielsen and Ninomiya, PRL **130**, 389 (1983)

Weyl semimetals

Chiral anomaly⁸

- Weyl point ($n = \pm 1$) in a magnetic field $\mathbf{B} = B\hat{\mathbf{e}}_z \rightarrow$ Landau levels⁹

$$E_n(k_z) = \begin{cases} \text{sgn}(n)v\sqrt{k_z^2 + 2|n|eB} & |n| \geq 1 \\ vk_z & n = 0 \end{cases}$$



⁸Son and Spivak, PRB **88**, 104412 (2013)

⁹Nielsen and Ninomiya, PRL **130**, 389 (1983)

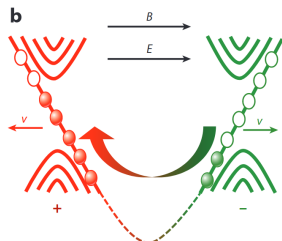
Weyl semimetals

Chiral anomaly⁸

- Weyl point ($n = \pm 1$) in a magnetic field $\mathbf{B} = B\hat{\mathbf{e}}_z \rightarrow$ Landau levels⁹

$$E_n(k_z) = \begin{cases} \text{sgn}(n)v\sqrt{k_z^2 + 2|n|eB} & |n| \geq 1 \\ vk_z & n = 0 \end{cases}$$

- slope of zeroth LL depends on the WP chirality (± 1)



⁸Son and Spivak, PRB **88**, 104412 (2013)

⁹Nielsen and Ninomiya, PRL **130**, 389 (1983)

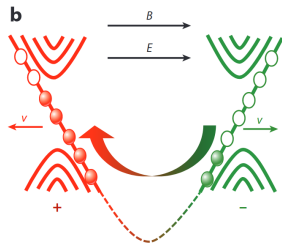
Weyl semimetals

Chiral anomaly⁸

- Weyl point ($n = \pm 1$) in a magnetic field $\mathbf{B} = B\hat{\mathbf{e}}_z \rightarrow$ Landau levels⁹

$$E_n(k_z) = \begin{cases} \text{sgn}(n)v\sqrt{k_z^2 + 2|n|eB} & |n| \geq 1 \\ vk_z & n = 0 \end{cases}$$

- slope of zeroth LL depends on the WP chirality (± 1)



- $\mathbf{E} \parallel \mathbf{B}$: charge conservation violated at individual WPs
 - charge pumped from one WP to another \rightarrow increased σ_{xx}

⁸Son and Spivak, PRB **88**, 104412 (2013)

⁹Nielsen and Ninomiya, PRL **130**, 389 (1983)

Weyl semimetals

Chiral anomaly¹⁰

- ▶ parabolic bands in magnetic field: positive longitudinal magnetoresistance
 - ▶ increased resistivity: $\Delta\rho_{zz}/\Delta B > 0$

¹⁰Son and Spivak, PRB **88**, 104412 (2013)

¹¹Xiong *et al.*, Science **350**, 413 (2015)

Weyl semimetals

Chiral anomaly¹⁰

- ▶ parabolic bands in magnetic field: positive longitudinal magnetoresistance
 - ▶ increased resistivity: $\Delta\rho_{zz}/\Delta B > 0$
- ▶ Weyl semimetal in magnetic field ($E \parallel B$): negative longitudinal magnetoresistance
 - ▶ decreased resistivity: $\Delta\rho_{zz}/\Delta B < 0$

¹⁰Son and Spivak, PRB **88**, 104412 (2013)

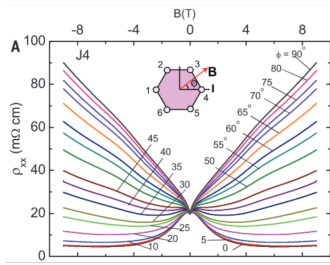
¹¹Xiong *et al.*, Science **350**, 413 (2015)

Weyl semimetals

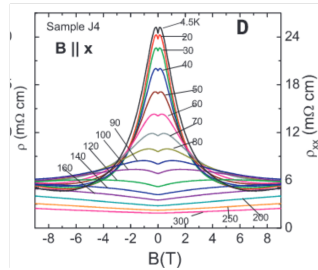
Chiral anomaly¹⁰

- ▶ parabolic bands in magnetic field: positive longitudinal magnetoresistance
 - ▶ increased resistivity: $\Delta\rho_{zz}/\Delta B > 0$
- ▶ Weyl semimetal in magnetic field ($E \parallel B$): negative longitudinal magnetoresistance
 - ▶ decreased resistivity: $\Delta\rho_{zz}/\Delta B < 0$
- ▶ Example: Na₃Bi¹¹

angle between E and B:



temperature:



¹⁰Son and Spivak, PRB **88**, 104412 (2013)

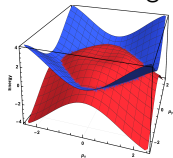
¹¹Xiong et al., Science **350**, 413 (2015)

Nodal-line semimetals

¹²Rauch *et al.*, PRB **96**, 235103 (2017)

Nodal-line semimetals

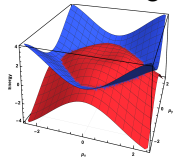
- ▶ band crossings along a line in the BZ¹²



¹²Rauch *et al.*, PRB **96**, 235103 (2017)

Nodal-line semimetals

- ▶ band crossings along a line in the BZ¹²

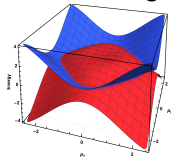


- ▶ often protected by symmetry (different IRREPs can cross)

¹²Rauch *et al.*, PRB **96**, 235103 (2017)

Nodal-line semimetals

- ▶ band crossings along a line in the BZ¹²

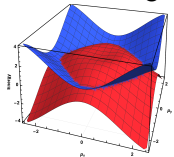


- ▶ often protected by symmetry (different IRREPs can cross)
- ▶ Berry phase along a line enclosing the NL: $\phi = \pi$

¹²Rauch *et al.*, PRB **96**, 235103 (2017)

Nodal-line semimetals

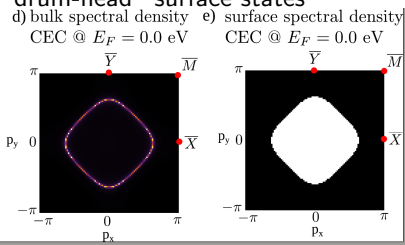
- ▶ band crossings along a line in the BZ¹²



- ▶ often protected by symmetry (different IRREPs can cross)
- ▶ Berry phase along a line enclosing the NL: $\phi = \pi$
- ▶ “drum-head” surface states

d) bulk spectral density e) surface spectral density

CEC @ $E_F = 0.0$ eV CEC @ $E_F = 0.0$ eV



¹²Rauch et al., PRB **96**, 235103 (2017)

Topological semimetals

Summary:

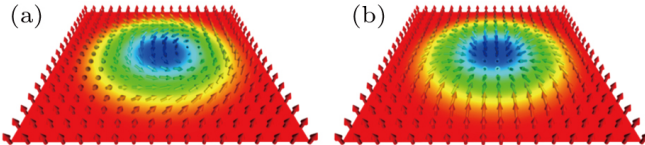
- ▶ band crossings at E_F
- ▶ Weyl or Dirac type
- ▶ crossings protected by symmetry
- ▶ typical surface states
- ▶ unusual transport properties
- ▶ ideally: only the crossings at E_F , no other bands

Magnetic skyrmions¹³

¹³Nagaosa and Tokura, Nature Nanotechnology **8**, 899 (2013)

Magnetic skyrmions¹³

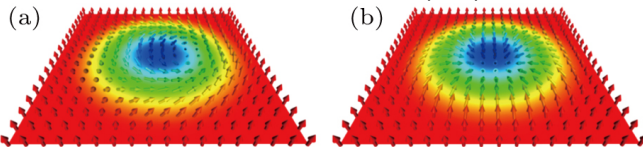
- ▶ non-coplanar real-space spin texture $\mathbf{n}(x, y)$



¹³Nagaosa and Tokura, Nature Nanotechnology **8**, 899 (2013)

Magnetic skyrmions¹³

- ▶ non-coplanar real-space spin texture $\mathbf{n}(x, y)$



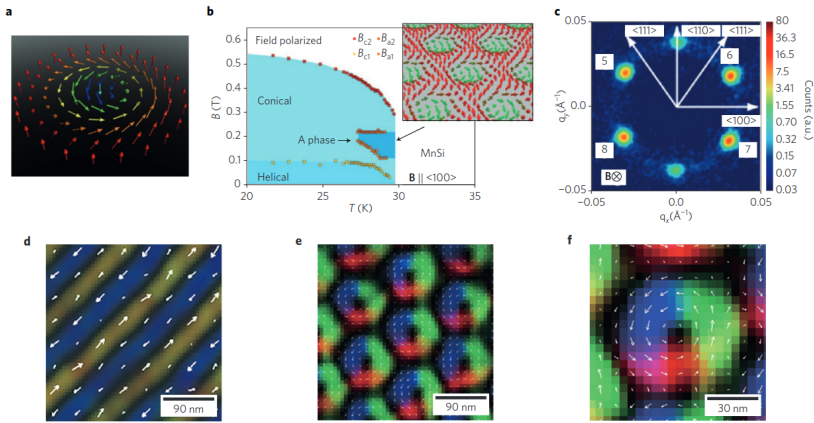
- ▶ topological invariant: skyrmion / winding number

$$N_{2D} = \frac{1}{4\pi} \iint d^2 r \mathbf{n} \cdot \left(\frac{\partial \mathbf{n}}{\partial x} \times \frac{\partial \mathbf{n}}{\partial y} \right)$$

- ▶ N_{2D} . . . integer
- ▶ no smooth transition from skyrmion ($N_{2D} = 1$) to FM ($N_{2D} = 0$)

¹³Nagaosa and Tokura, Nature Nanotechnology **8**, 899 (2013)

Magnetic skyrmions¹³



- ▶ small-angle neutron scattering: reciprocal space
- ▶ Lorentz transmission electron microscopy: real space
- ▶ spin-resolved scanning tunnelling microscopy: real space

¹³Nagaosa and Tokura, Nature Nanotechnology **8**, 899 (2013)

Magnetic skyrmions¹⁵

- ▶ localized objects - both individual or on a lattice
- ▶ topologically protected

¹⁴Back *et al.*, J. Phys. D: Appl. Phys. **53**, 363001 (2020)

¹⁵Nagaosa and Tokura, Nature Nanotechnology **8**, 899 (2013)

Magnetic skyrmions¹⁵

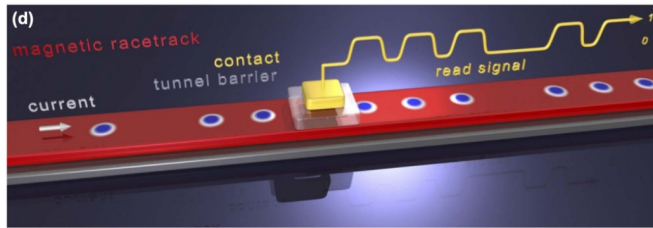
- ▶ localized objects - both individual or on a lattice
- ▶ topologically protected
- ▶ can be manipulated by external stimuli (static fields, laser)
 - ▶ creation / annihilation
 - ▶ movement

¹⁴Back *et al.*, J. Phys. D: Appl. Phys. **53**, 363001 (2020)

¹⁵Nagaosa and Tokura, Nature Nanotechnology **8**, 899 (2013)

Magnetic skyrmions¹⁵

- ▶ localized objects - both individual or on a lattice
- ▶ topologically protected
- ▶ can be manipulated by external stimuli (static fields, laser)
 - ▶ creation / annihilation
 - ▶ movement
- ▶ application as information carrier^{14?}
- ▶ manipulation cheaper than in electronics?



¹⁴Back *et al.*, J. Phys. D: Appl. Phys. **53**, 363001 (2020)

¹⁵Nagaosa and Tokura, Nature Nanotechnology **8**, 899 (2013)

Majorana fermions¹⁶

¹⁶Elliott and Franz, Rev. Mod. Phys. **87**, 137 (2015)

Majorana fermions¹⁶

Particle physics view

Dirac equation $(i\gamma^\mu \partial_\mu - m)\Psi = 0$ with non-unique matrices γ^μ

¹⁶Elliott and Franz, Rev. Mod. Phys. **87**, 137 (2015)

Majorana fermions¹⁶

Particle physics view

Dirac equation $(i\gamma^\mu \partial_\mu - m)\Psi = 0$ with non-unique matrices γ^μ

- ▶ Dirac representation matrices
 - ▶ complex solution
 - ▶ describes particle and antiparticle pair, both spin 1/2

¹⁶Elliott and Franz, Rev. Mod. Phys. **87**, 137 (2015)

Majorana fermions¹⁶

Particle physics view

Dirac equation $(i\gamma^\mu \partial_\mu - m)\Psi = 0$ with non-unique matrices γ^μ

- ▶ Dirac representation matrices
 - ▶ complex solution
 - ▶ describes particle and antiparticle pair, both spin 1/2
- ▶ Majorana representation matrices
 - ▶ real solution
 - ▶ Majorana equation decouples into two independent systems
 - ▶ each solution: neutral particle, spin 1/2,
no distinction between particle and antiparticle → Majorana f.
 - ▶ Can each system exist individually?

¹⁶Elliott and Franz, Rev. Mod. Phys. **87**, 137 (2015)

Majorana fermions¹⁷

Solid-state physics view

Fermionic creation and annihilation operators: c_j^\dagger, c_j

anticommutation relations $\{c_i^\dagger, c_j^\dagger\} = \{c_i, c_j\} = 0, \{c_i^\dagger, c_j\} = \delta_{ij}$

¹⁷Elliott and Franz, Rev. Mod. Phys. **87**, 137 (2015)

Majorana fermions¹⁷

Solid-state physics view

Fermionic creation and annihilation operators: c_j^\dagger, c_j

anticommutation relations $\{c_i^\dagger, c_j^\dagger\} = \{c_i, c_j\} = 0, \{c_i^\dagger, c_j\} = \delta_{ij}$

► transformation to Majorana basis:

$$c_j = \frac{1}{2} (\gamma_{j1} + i\gamma_{j2}) \quad \gamma_{j1} = c_j^\dagger + c_j$$

$$c_j^\dagger = \frac{1}{2} (\gamma_{j1} - i\gamma_{j2}) \quad \gamma_{j2} = i(c_j^\dagger - c_j)$$

► $\{\gamma_{i\alpha}, \gamma_{j\beta}\} = 2\delta_{ij}\delta_{\alpha,\beta}, \gamma_{i\alpha}^\dagger = \gamma_{i\alpha}$

¹⁷Elliott and Franz, Rev. Mod. Phys. **87**, 137 (2015)

Majorana fermions¹⁷

Solid-state physics view

Fermionic creation and annihilation operators: c_j^\dagger, c_j

anticommutation relations $\{c_i^\dagger, c_j^\dagger\} = \{c_i, c_j\} = 0, \{c_i^\dagger, c_j\} = \delta_{ij}$

► transformation to Majorana basis:

$$c_j = \frac{1}{2} (\gamma_{j1} + i\gamma_{j2}) \quad \gamma_{j1} = c_j^\dagger + c_j$$

$$c_j^\dagger = \frac{1}{2} (\gamma_{j1} - i\gamma_{j2}) \quad \gamma_{j2} = i(c_j^\dagger - c_j)$$

- $\{\gamma_{i\alpha}, \gamma_{j\beta}\} = 2\delta_{ij}\delta_{\alpha,\beta}, \gamma_{i\alpha}^\dagger = \gamma_{i\alpha}$
- each Dirac particle is a superposition of two Majoranas
- each Majorana is a superposition of a particle and an antiparticle
- **task: separate both Majoranas spatially**

¹⁷Elliott and Franz, Rev. Mod. Phys. **87**, 137 (2015)

Majorana fermions¹⁷

Solid-state physics view

Fermionic creation and annihilation operators: c_j^\dagger, c_j

anticommutation relations $\{c_i^\dagger, c_j^\dagger\} = \{c_i, c_j\} = 0, \{c_i^\dagger, c_j\} = \delta_{ij}$

► transformation to Majorana basis:

$$c_j = \frac{1}{2} (\gamma_{j1} + i\gamma_{j2}) \quad \gamma_{j1} = c_j^\dagger + c_j$$

$$c_j^\dagger = \frac{1}{2} (\gamma_{j1} - i\gamma_{j2}) \quad \gamma_{j2} = i(c_j^\dagger - c_j)$$

- $\{\gamma_{i\alpha}, \gamma_{j\beta}\} = 2\delta_{ij}\delta_{\alpha,\beta}, \gamma_{i\alpha}^\dagger = \gamma_{i\alpha}$
- each Dirac particle is a superposition of two Majoranas
- each Majorana is a superposition of a particle and an antiparticle
- **task: separate both Majoranas spatially**
- search in superconductors ($e^- - h^+$ superpositions in BCS theory)
- similar to excitons, but excitons are bosons

¹⁷Elliott and Franz, Rev. Mod. Phys. **87**, 137 (2015)

Majorana fermions¹⁸

1D model: Kitaev chain

- ▶ spinless fermions on a 1D lattice"

$$H = \sum_j \left[-t(c_j^\dagger c_{j+1} + H.c.) - \mu \left(c_j^\dagger c_j - \frac{1}{2} \right) + (\Delta c_j^\dagger c_{j+1}^\dagger + H.c.) \right]$$

t . . . hopping amplitude, Δ . . . nearest-neighbour pairing amplitude,
 μ . . . chemical potential

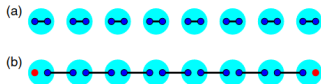
¹⁸Elliott and Franz, Rev. Mod. Phys. **87**, 137 (2015)

Majorana fermions¹⁸

1D model: Kitaev chain

- ▶ Majorana basis, $\Delta = t = 0$ (a):

$$H = \frac{i}{2}(-\mu) \sum_j \gamma_{j,1} \gamma_{j,2} = -\mu \sum_j \left(c_j^\dagger c_j - \frac{1}{2} \right)$$



¹⁸Elliott and Franz, Rev. Mod. Phys. **87**, 137 (2015)

Majorana fermions¹⁸

1D model: Kitaev chain

- ▶ Majorana basis, $\Delta = t = 0$ (a):

$$H = \frac{i}{2}(-\mu) \sum_j \gamma_{j,1} \gamma_{j,2} = -\mu \sum_j \left(c_j^\dagger c_j - \frac{1}{2} \right)$$

- ▶ Majorana basis, $\Delta = t, \mu = 0$ (b):

$$H = it \sum_j \gamma_{j,2} \gamma_{j+1,1} = 2t \sum_{j=1}^{N-1} \left(a_j^\dagger a_j - \frac{1}{2} \right)$$

with fermion operators $a_j = \frac{1}{2}(\gamma_{j,2} + i\gamma_{j+1,1})$, $a_j^\dagger = \frac{1}{2}(\gamma_{j,2} - i\gamma_{j+1,1})$



(b) unpaired Majoranas at the ends

¹⁸Elliott and Franz, Rev. Mod. Phys. **87**, 137 (2015)

Majorana fermions¹⁹

- ▶ “topological superconductors”
 - ▶ unpaired Majorana modes guaranteed at the edges

¹⁹Elliott and Franz, Rev. Mod. Phys. **87**, 137 (2015)

Majorana fermions¹⁹

- ▶ “topological superconductors”
 - ▶ unpaired Majorana modes guaranteed at the edges
- ▶ realization (ideas): non-degenerate bands necessary
 - ▶ edge of a 2D TI + superconductivity
 - ▶ semiconductor quantum wires
 - ▶ parabolic band
 - ▶ spin-orbit coupling (broken I)
 - ▶ superconductivity

¹⁹Elliott and Franz, Rev. Mod. Phys. **87**, 137 (2015)

Majorana fermions¹⁹

- ▶ “topological superconductors”
 - ▶ unpaired Majorana modes guaranteed at the edges
- ▶ realization (ideas): non-degenerate bands necessary
 - ▶ edge of a 2D TI + superconductivity
 - ▶ semiconductor quantum wires
 - ▶ parabolic band
 - ▶ spin-orbit coupling (broken I)
 - ▶ superconductivity
- ▶ envisioned application: quantum computing
 - ▶ N Dirac fermions composed of delocalized Majorana pairs:
state vector $|\Psi\rangle$
 - ▶ nonlocal storing of quantum bits → large coherence time
 - ▶ exchanges of positions of Majorana zero modes:
 - non-commutative transformation of the state vector
 - “topologically” protected final state after a sequence of exchanges

¹⁹Elliott and Franz, Rev. Mod. Phys. **87**, 137 (2015)

Conclusion

- ▶ Higher-order topological insulators
- ▶ Dirac semimetals
- ▶ Weyl semimetals
- ▶ nodal-line semimetals
- ▶ magnetic skyrmions
- ▶ Majorana fermions

Following seminar:

1. Envisioned applications, promises, expectations?
2. Closing discussion
3. Questions, remarks